High-efficiency photochemical hole burning for an infrared color center

W. E. Moerner, F. M. Schellenberg, and G. C. Bjorklund

IBM Research Laboratory, San Jose, California 95193

Prasad Kaipa and Fritz Lüty

Physics Department, University of Utah, Salt Lake City, Utah 84112

(Received 12 November 1984)

The photochemical hole-burning properties of the 8892-Å zero-phonon-line defect absorption in electron-irradiated NaF:OH$^-$ and NaF:Mn^{2+} at liquid-helium temperatures are described and analyzed. This system is the first reported example of high-efficiency (10^{-2}) hole burning for a color center in alkali halides. Although the width of the inhomogeneously broadened line increases linearly as the OH$^-$ concentration is varied by a factor of 25, the hole width extrapolated to zero burning power remains essentially constant at 1.65±0.15 GHz over the same range. In contrast to most other color centers, holes can be burned 100% deep in this system, which suggests the absence of strong reverse reactions. A kinetic model for hole-growth data is presented that includes the effects of the homogeneous line shape and the dependence of the density of centers and burning flux upon distance into the sample. The hole-growth dynamics follow first-order kinetics quite well over two decades in time indicating that the quantum efficiency is essentially constant for all centers. This is evidence that the hole-burning process involves electron tunneling over a well-defined single barrier.

I. INTRODUCTION

Persistent spectral holes in the absorption lines of inhomogeneously broadened optical transitions in solids have been proposed as data elements in a frequency-domain optical information storage system.[1] Scientifically, low-temperature spectral hole burning is an important probe of host-impurity interactions, dephasing interactions, and site-selective photochemistry.[2-4] Because of these two facts, the properties of new host-defect combinations exhibiting photochemical or photophysical hole burning are of significant interest in both the scientific and technological communities.

Aggregate color centers in ionic solids provide a large number of zero-phonon optical transitions[5] spanning a wide wavelength range that may be studied for photochemical hole burning (PHB). The first example of PHB in a color center was provided by the F_3^+ center in NaF at 5456 Å.[6] Since that time, PHB has been studied in a number of other color centers in the visible range.[7,8] Recently, PHB was discovered in the infrared color center composed of $R'(F_3^-)$ defects in LiF at 8330 Å,[9] and for the first time holes have been read and written with a GaAlAs diode laser in this system.[10] The hole-burning process in these materials is thought to be the photoinduced tunneling of an electron from the color center to a nearby trap.

However, the PHB in color centers reported to date[11] has exhibited extremely low burning efficiency, where the burning efficiency η is defined as the branching ratio for photochemistry compared to all other deexcitation processes, or equivalently, the probability for hole burning per center per photon absorbed.[12] This definition means that η is equal to 1 over the number of photons that must be absorbed by a single center before photochemistry

occurs. For all the color centers mentioned above, η is disappointingly low: 10^{-6} to 10^{-7}. One may ask the following question: Is this low efficiency intrinsic to PHB in color centers? The answer to such a question may lead to a better understanding of the microscopic processes responsible for PHB. Moreover, for optical storage applications it is important that high-efficiency processes be studied, because for constant burning time, lower photon fluxes will be required for writing holes in high-efficiency systems compared to those for low-efficiency systems.

In this work we describe the properties of PHB for a new defect system: the 8892-Å color center in electron-irradiated NaF:OH$^-$ and NaF:Mn^{2+} single crystals.[13] The production and incoherent bleaching characteristics of this center have been described in a separate publication[14] in which evidence is presented that the center may be an F_4^- aggregate. In contrast to previously studied color centers, the burning efficiency for this system is quite large—near 10^{-2}. In addition, holes may be burned 100% deep in this system, in contrast to the 10% to 20% limiting hole depths for almost all other color centers.[15] We report the systematics of the observed PHB, including hole linewidths, effects of varying OH$^-$ concentration, and hole-growth dynamics. The hole linewidth [full width at half maximum (FWHM)] extrapolated to zero burning time is 1.65±0.15 GHz at 1.4 K for all concentrations of OH$^-$ ions studied, even though the width of the zero-phonon-line absorption increases approximately linearly with OH$^-$ concentration. We present a detailed kinetic model for the hole-growth data that includes the effects of off-resonance molecules as well as the spatial variation of center density and light flux with distance into the sample. To a good approximation, the hole dynamics can be explained by assuming a constant quantum efficiency for all centers. The observation of high-

efficiency hole burning in an infrared color center proves that low quantum efficiencies and shallow holes are not intrinsic to PHB in color-center zero-phonon lines.

II. EXPERIMENTAL DETAILS

The samples used for these studies were Kyropolous-grown single crystals of NaF doped with OH^- ions or Mn^{2+} ions by the addition of NaOH or MnF_2 to the melt. The presence of OH^- ions in the host crystal greatly enhances the production of the 8892-Å color center; in particular, in pure NaF only very weak 8892-Å absorption lines are produced, even with extended electron irradiation times. The addition of Mn^{2+} ions to the crystal also enhances the production of the 8892-Å color center in a similar fashion. Since no difference was observed between the hole-burning properties in the NaF:Mn^{2+} host compared to the NaF:OH^- host, the bulk of this paper will concentrate on the NaF:OH^--host data. The Mn^{2+} data only serve to show that the hole-burning properties reported in this paper cannot be attributed to special characteristics of the OH^- ion, for example, the OH^- dipole moment. Samples were cleaved from the as-grown boules and colored by exposure to an intense electron beam as described elsewhere.[14] Most samples had peak absorption coefficients in the range 1.0–3.0 cm^{-1}. Relative OH^- concentrations were determined by measuring the strength of the OH^- infrared transition at 2.68 μm. Due to the extreme light sensitivity of the colored samples, the crystals were stored at 77 K in the dark after electron irradiation.

Two types of experiments were conducted: broadband, low-intensity linear spectroscopy to examine inhomogeneous line shapes, and narrow-band laser experiments to probe the hole-burning properties. All measurements were performed in the temperature range 1.4–2 K in a superfluid liquid-helium immersion cryostat. Zero-phonon-line (ZPL) line-shape studies were performed with chopped light from a tungsten lamp filtered by a 0.75-m monochromator with 50-μm slits. Since even the infrared radiation from a small pen light was found to bleach the ZPL in a few seconds at low temperatures, the samples were aligned using a diffuse He-Ne laser for overall illumination and yellow light from the monochromator for focused illumination. The crystals were not exposed to light in the 750–889-nm range until the start of data acquisition. The transmitted light was detected with a silicon photodiode and a lock-in amplifier. We observed that for this high-efficiency system, the use of "white light" spectroscopy, in which broadband light from a lamp passes through the sample *before* dispersion in a monochromator, causes severe bleaching of the ZPL before the absorption due to the ZPL can be detected.

Hole-burning measurements were performed in transmission using a frequency-stabilized, Kr^+-ion-laser-pumped, LDS-821 (Styryl-9, Exciton Chemical Company) dye laser with a 3-MHz linewidth. Due to the high hole-burning quantum efficiency for the 8892-Å color center, a special technique was found to be essential for hole detection. We found that extremely low probing laser powers were necessary in order to prevent the formation of a "trench" in the absorption line due to the burning of all
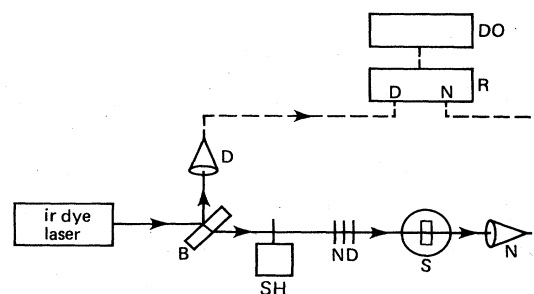
FIG. 1. Schematic arrangement for precision ratiometric hole-burning spectroscopy. Legend: B—beamsplitter, SH—shutter, ND—neutral-density filters, S—sample in low-temperature optical cryostat, N—numerator detector and preamplifier, D—denominator reference detector, R—precision ratiometer, DO—digital-averaging oscilloscope.

the centers in the range of the laser scan. Figure 1 schematically shows the experimental arrangement. The ir laser beam was split into a reference beam for detector D and a sample beam. The sample beam was controlled by a mechanical shutter SH and attenuated by neutral-density filters ND before impinging on the sample S in a liquid-helium cryostat. Probe powers in the 100 pW–1-nW range in a 625-μm diameter spot were found to produce negligible deterioration of the holes during the 20- to 30-s period required for detection. However, scanning powers in the 10–20-nW range could also be used for detection, if the spectrum was acquired during the first one or two laser scans after the start of the reading process (time for one laser scan=0.25 s). The transmitted beam was detected with a high-sensitivity detector N, composed of a silicon photodiode and a low-noise field-effect transistor (FET) preamplifier. The laser power measured by the N detector was normalized to that measured by the D detector using a precision, high-dynamic-range ratiometer R. Both detectors and the ratiometer were constructed with an 80-kHz electrical bandwidth to assure accurate ratio determination at high laser scan rates. However, the output of the ratiometer was filtered with a 1-ms time constant before further processing. Hole spectra were averaged with a digital oscilloscope DO. This precision ratiometric measurement technique[16] was found to be essential for the detection of holes in this high-efficiency system. Fluorescence excitation could not be used due to the high scanning powers required in order to detect the weak infrared fluorescence from this center.

III. STATICS: LINEWIDTHS AND MAXIMUM HOLE DEPTH

Figure 2 shows a transmission spectrum at 1.4 K of the inhomogeneously broadened ZPL. The wavelength scale was calibrated using radiation from the dye laser and a Burleigh WA-10 wavemeter. The ZPL full-width-at-half maximum absorption for this sample, 4.1 Å, is comparable to that observed for other F aggregate centers in alkali halides.[5] However, for this color center the possibility exists of altering the width of the inhomogeneous line by varying the OH^- doping. Figure 3 (solid line, solid
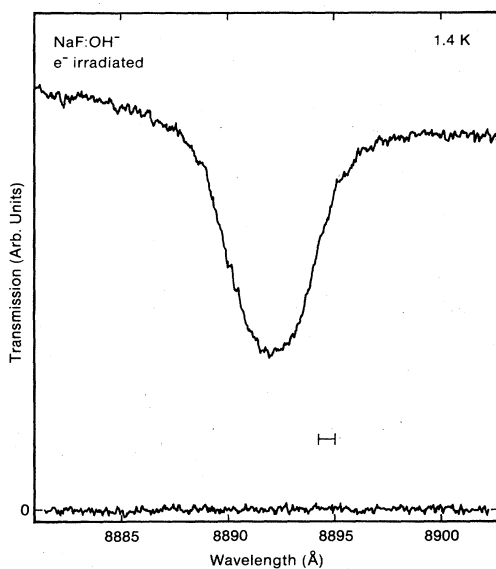
FIG. 2. Transmission spectrum of electron-irradiated NaF:OH⁻ at 1.4 K. The spectrometer resolution is indicated. The relative OH⁻ concentration is approximately 0.2.

circles, left axis) shows that the ZPL FWHM linewidth increases by almost a factor of 2 with a 25-fold increase in OH⁻ concentration. The linewidth depends linearly on concentration with a coefficient of determination of 0.94. Over the same range of OH⁻ concentration, the peak absorption coefficient drops by approximately a factor of 4 for samples with constant electron-beam exposure during coloring. Thus, the integrated absorption strength falls slightly with increasing OH⁻ concentration, indicating that large concentrations of OH⁻ ions may partially inhibit the formation of the defect center during the coloring process. As was remarked above, however, the presence of OH⁻ ions is important for the formation of large con-
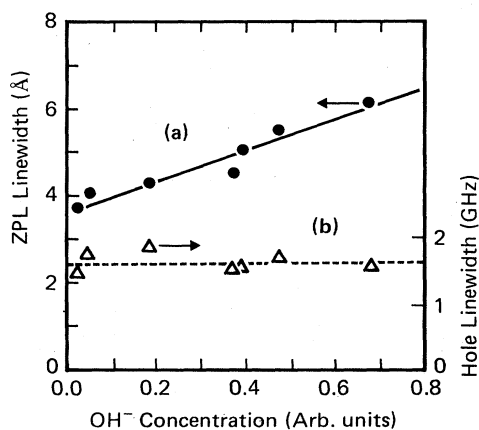
FIG. 3. Inhomogeneous zero-phonon-line (ZPL) linewidth full width at half maximum (FWHM) and photochemical hole linewidth (FWHM) versus relative OH⁻ concentration at 1.4 K. The solid circles and solid line refer to the ZPL linewidth (left axis), and the open triangles and dashed line refer to the hole linewidth (right axis).
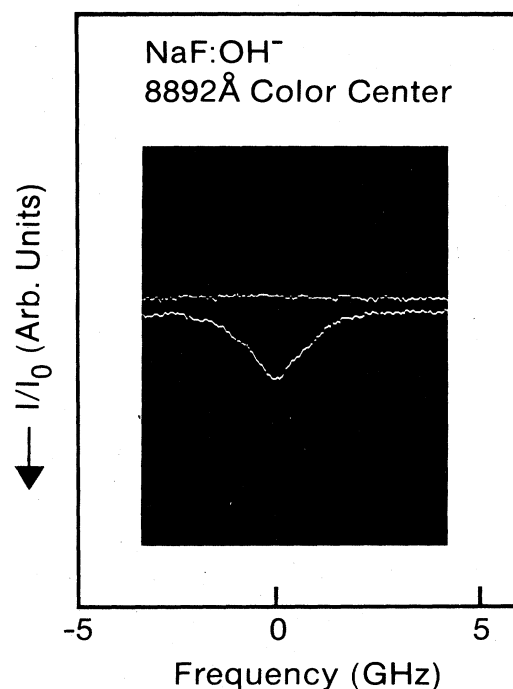
FIG. 4. Spectrum of a typical photochemical hole in the NaF:OH⁻ system at 1.4 K (lower curve). The sample absorption before hole burning is also indicated (upper curve). Two scans were averaged to produce this trace.

centrations of the color center from the outset. Apparently, the enhancing effect of OH⁻ ions on the growth of the 8892-Å center saturates at some low concentration of the ion, and at larger concentrations, an inhibiting mechanism appears. Nevertheless, some applications require the largest possible ratio of inhomogeneous ZPL width to hole width, a fact which makes the study of heavily doped crystals especially interesting.

Turning now to the photochemical hole-burning results, Fig. 4 shows a hole burned with approximately 5 nW of laser power in a 1.5-mm-diameter spot with the laser frequency held constant for 5 s. The hole was detected with the same power level in two scans of the laser (0.25 s each) to prevent burning of the entire frequency region near the hole. The hole width extrapolated to zero burning time and averaged over measurements in seven samples is 1.65±0.15 GHz FWHM. The implications of this measured hole width will be discussed below.

In contrast to the shallow steady-state holes observed with most other color centers[15] and also with photophysical systems,[3] holes can be burned 100% deep in this color center, indicating that strong reverse photoreactions are not present. Apparently, the photoinduced change involves a direct alteration of the center itself, rather than a photophysical alteration of the surrounding environment. The hole lifetime is very long, showing less than a 10% decay after hours in the dark at 2 K. Temperature-dependent studies of the linewidth and hole annealing were not performed; however, the holes definitely disappeared after temperature cycling to room temperature.

We observed that part of the integrated ZPL absorption strength disappears after hole burning at low temperatures and subsequent temperature cycling. This observation is consistent with the broadband bleaching experiments,[14] and suggests that the apparent "hole annealing" is not a complete reversal of the photochemistry, but rather a partial redistribution of the unburned centers due to strain relaxation. The deep steady-state holes and the partial permanence of the photochemistry after temperature cycling are consistent with the model that the hole-burning mechanism is ionization of the excited center due to electron tunneling to a deep nearby trap. The question of whether or not there is a distribution of traps will be discussed below.

The observed low-power hole linewidth of 1.65 GHz is somewhat anomalous. This hole width is much larger than the 30—50-MHz hole widths observed for other aggregate color centers in NaF.[6-8] Hole widths for most color centers have been lifetime limited, and in order for the 8892-Å center to have a T_1 limited hole width, strong nonradiative processes must be controlling the excited-state decay. We show below that the photochemical (and hence nonradiative) pathway out of the excited state is quite efficient. It may therefore be possible that the reaction channel itself is partially responsible for the small value of T_1. If the weak infrared fluorescence from this center could be measured adequately, exact values for T_1 could be determined which might help illuminate the mechanisms responsible for the large hole widths.

Another possible explanation for the large hole width might be defect-induced dephasing caused by the presence of OH^- or Mn^{2+} ions near the center. To test this hypothesis, low-power-limiting hole widths were determined for a variety of samples with varying OH^- concentrations. Figure 3 (open triangles, right axis, dashed line) shows the measured hole widths as a function of relative OH^- concentration. The hole width is approximately 1.65 ± 0.15 GHz, independent of OH^- concentration. Unfortunately, the hole width in pure NaF crystals could not be measured due to the extremely weak 8892-Å absorption that is observed in such hosts. We may only conclude that varying the concentration of OH^- ions by a factor of 25 does not appreciably affect the width of the photochemical holes. It is still possible that the presence of even small concentrations of OH^- ions produces a fixed amount of dephasing which gives rise to the observed hole widths. However, since similar hole widths are observed with Mn^{2+} doping, we may at least conclude that the additional dephasing is not due to the OH^- dipole, for instance. In addition, since Mn^{2+} ions enter the lattice in conjunction with a vacancy to maintain charge neutrality (as opposed to the case with OH^- ions), large local electric fields are also not responsible for the broad hole widths.

IV. DYNAMICS: HOLE GROWTH AND EFFICIENCY

Hole-growth curves provide another way to characterize the burning process in this system. If the hole-growth characteristic can be measured accurately, comparison with a theoretical growth curve can provide information

about the hole-burning mechanism.[3] For these measurements, a somewhat larger-than-normal intensity for the probing beam was used, and the growing sample transmission produced by the probing laser beam was recorded in real time. To reduce the noise from low-frequency drifts, the probing beam was chopped at 1.04 kHz and detected with a lock-in amplifier with a 125-ms time constant. Figure 5 shows a trace of the time-varying sample transmission for a probe laser intensity of 5.6 $\mu W/cm^2$. To perform this measurement, the sample was cooled to 2 K in the dark, and the probe laser was unblocked at time $t=0$. The signal transmitted through the sample begins at a value reflecting the sample transmission in the absence of a hole and then grows slowly over many seconds. This measurement corresponds to line-center burning and simultaneous detection of the resulting hole with a single laser. The hole widths measured at various burning times are indicated on the curve. These hole widths were determined during similar hole-growth measurements by interrupting the burning process, attenuating the probe beam, and scanning the hole spectrum. The hole broadens due to photochemical saturation,[17] underscoring the essential requirement that the intrinsic hole width occurs only in the zero-burning-time limit. In essence, as those centers in resonance with the laser are removed from the inhomogeneous line, centers further from the laser wavelength eventually undergo photochemistry as well due to absorption in the Lorentzian tails. This process will be modeled in detail below.

The initial slope of the growth curve in Fig. 5 may be used to estimate the hole-burning quantum efficiency η.[3,12] A natural definition for η is

$$\eta = \frac{-[dN_v(t)/dt]\,|_{t=0}V}{(P/h\nu)(1-T_0-R)} = \frac{[dT(t)/dt]\,|_{t=0}}{\sigma T_0(I/h\nu)(1-T_0-R)} \; ,$$

$$(1)$$

where N_v is the density of centers within a homogeneous linewidth of the laser frequency, V is the volume of sample irradiated by the laser, P is the incident laser power, ν is the laser frequency, T_0 is the initial sample transmission (external transmittance), R is the total reflection loss,
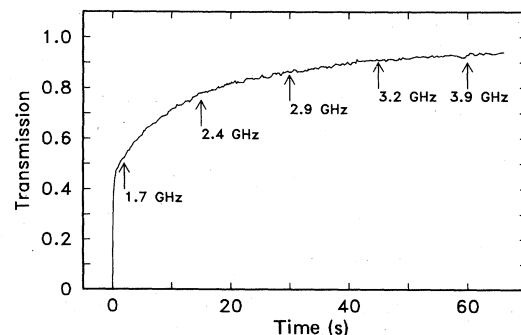
FIG. 5. Hole-growth curve as a function of time after laser unblocking at $t=0$. The hole widths (FWHM) at various burning times are indicated. The chopping frequency was 1.04 kHz and the lock-in time constant was 125 ms. The sample length was 0.165 cm.

h is Planck's constant, $T(t)$ is the time-varying sample transmission, I is the average incident laser intensity, and σ is the cross section. Thus, the slope of the hole-growth curve at $t=0$ can be used to compute the initial rate of change of N_v, if the cross section σ is known. Proper calculation of the low-temperature cross section requires knowledge of either the dipole moment or the oscillator strength of the transition. Since the 8892-Å color center is relatively new, neither of these quantities is known with precision. We make the approximation that the oscillator strength for the entire transition is of order 0.1. This is a reasonable assumption for aggregate color centers, in that common oscillator strengths for F centers and M centers are 0.8 and 0.2, respectively.[18] This oscillator strength is divided between the ZPL and the phonon sideband at low temperatures. By integrating the measured[14] absorption curves for the ZPL and phonon sideband, we find that roughly $\frac{1}{5}$ of the absorption strength may be attributed to the ZPL, so we take $f=0.02$. Using the following expression[12] for the peak cross section in one homogeneous packet,

$$\sigma = \frac{2\pi e^2 T_2}{cm_e} \left[\frac{L}{n} \right] f , \qquad (2)$$

where e is the electron charge, m_e is the electron mass, T_2 is the homogeneous relaxation time determined from $T_2 = 2/\pi \Delta \nu_{hole}$, n is the index of refraction, $L = [(n^2+2)/3]^2$, and c is the speed of light, we find $\sigma = 4.8 \times 10^{-13}$ cm^2. Using the measured values $dT(t)/dt_{t=0} = 42 \times 10^{-3}$ and $I = 5.6$ μW/cm^2 the resulting value for η is 1.5×10^{-2}. Of course, the approximate value for the oscillator strength used in this calculation and the Gaussian shape of the laser beam make this estimate useful only to within perhaps a factor of 2 or 3. Nevertheless, this quantum efficiency is easily several orders of magnitude larger than the 10^{-6} to 10^{-7} quantum efficiencies observed for other color centers reported to date.[6-9,11]

One way to learn about the underlying mechanism responsible for hole formation would be to fit the hole-growth curve in Fig. 5 using a phenomenological model. As opposed to the near-exponential growth curves observed when the ZPL is bleached with broadband light from a monochromator,[14] this hole-growth curve is clearly nonexponential with a fast rate at short times and slower and slower rates at longer times. This may be caused by the increase in hole width with burning time (i.e., photochemical saturation, mentioned above) and by the nonuniform burning intensity resulting from faster bleaching of the centers on the side of the sample closer to the laser compared to the centers on the side of the sample further from the laser. In addition, growth curves with fast rates at short times and slow rates at long times can be caused by a distribution of quantum efficiencies for the various centers.[3] In effect, the centers with small barriers burn first, and at longer and longer times those centers with higher barriers undergo a photoinduced change as well.

To distinguish between these various possibilities, we have performed a kinetic analysis of the hole formation process. We use a first-order photochemical model for the hole-burning mechanism where we assume that the product is transparent at the laser frequency. The goal is to produce a theoretical prediction for the hole-growth curve shown in Fig. 5. The problem is complicated by the fact that the values of optical density used here cause centers at the front of the sample to experience a larger burning flux than those at the rear of the sample. As a result, the spatial dependence of the local variables along the direction of propagation x has to be taken into account in a self-consistent fashion. We compute the effect of the laser excitation upon each homogeneous class of centers in the inhomogeneously broadened line as a function of time, detuning from the burning laser, and distance into the sample. This is in effect a generalization of the elegant treatment of first-order photochemical reaction dynamics in an optically dense, homogeneously broadened medium presented by Simmons[19] and a density matrix treatment of the hole-burning problem for an inhomogeneously broadened transition in an optically thin sample presented by de Vries and Wiersma.[17]

We assume that the burning laser beam is at optical (radian) frequency $\omega = 0$, and that the laser power is low enough that the dynamics may be treated by rate equations. The laser beam is turned on at $t=0$, and we measure the transmitted power as a function of time at the end of the sample. The laser flux (in photons/s cm^2) at position x and time t in the sample is represented by $F(x,t)$. Each class of absorbing centers is indexed by the center frequency of the class ω and since the laser is at $\omega = 0$, the detuning of a given class from the laser is also ω. We represent the density of centers at x and t with center frequency ω by $N(x,t,\omega)$. With these definitions, the dynamics of the sample are completely determined by the following coupled, nonlinear differential equations:

$$\frac{dN(x,t,\omega)}{dt} = -\eta_P \left[\frac{\sigma}{1+(\omega/\Gamma)^2} \right] F(x,t)N(x,t,\omega) , \qquad (3)$$

$$\frac{dF(x,t)}{dx} = -\sigma \left[\frac{\Gamma}{\pi} \int_{-\infty}^{\infty} \frac{d\omega}{\Gamma^2+\omega^2} N(x,t,\omega) \right] F(x,t) , \qquad (4)$$

where η_P is the peak quantum efficiency[20] for centers exactly in resonance $(\eta_P = 2\eta)$, σ is the peak cross section, and 2Γ is the homogeneous linewidth (FWHM) for the transition. Equation (3) states that centers at ω are not affected by the full laser flux at $\omega = 0$, rather, they interact with the flux with the usual Lorentzian line shape. Equation (4) states that the local "absorption coefficient" for the laser at $\omega = 0$ is a convolution of the density of centers (at various detunings ω) times the Lorentzian absorption profile for each class. (The inhomogeneous line is assumed featureless on the frequency scale defined by Γ.) We note that the Gaussian transverse distribution of the laser beam is neglected. Inclusion of the Gaussian cross section would probably cause a slower initial hole growth, but then produce a larger slope at large times. Methods exist for the decomposition of Gaussian averaged transmittances,[21] but inclusion of these effects here unnecessarily complicates the analysis, and is unwarranted due to the already large uncertainties in the cross section.

These coupled equations can only be solved numerically. We chose to use an Adams-Moulton predictor-corrector method that had previously been found useful in modeling photon echo decays in optically thick media.[22] The integration was carried out on a three-dimensional grid of (x,t,ω) values. (In actuality, the frequency integrals were evaluated as a function of ω/Γ, so no particular value of Γ was required for the calculation.) The density N is known for all points on the $t=0$ plane, $N(x,0,\omega)=N_0$, where N_0 is the initially uniform density of centers. Similarly, the flux is known for all points on the $x=0$ plane, $F(0,t)=F_0$, where F_0 is the incident flux. The integration was performed using Eq. (3) as a propagator for the density function (along the t axis) and Eq. (4) as a propagator for the flux function (along the x axis). Several special cases had to be considered, because the first step along either axis had to performed with the value of the function known only at one previous grid point. For the general point, simultaneous steps along the x and t axes were made in order to maintain the logic of the predictor-corrector algorithm. Of course, at each point in the (x,t) plane, Eq. (3) was propagated for all values of ω, and then an appropriate integral over ω was performed in order to provide the value of the expression in brackets in Eq. (4). In this manner, the local variables $N(x,t,\omega)$ and $F(x,t)$ were determined for all times, positions, and detunings from the laser frequency. The total sample transmission was then calculated using $T(t)=F(x=L,t)/F_0$, where L is the sample length.

The results of the numerical solution of Eqs. (3) and (4) are represented by the solid line in Fig. 6. The points in the figure are the measured values of the sample transmission from Fig. 5. Several measured parameters were used to compute this fit: the flux entering the sample (neglecting small reflection losses) $F_0=2.51\times10^{13}$ photons/s cm^2 and the sample transmission before hole burning, $T_0=0.41$. The two microscopic parameters σ and η_P were varied to produce the fit. Variations in σ produce vertical shifts in the region near $t=0$ because this parameter along with T_0 actually determines N_0. Variations in η_P roughly shift the curve up and down at long times.
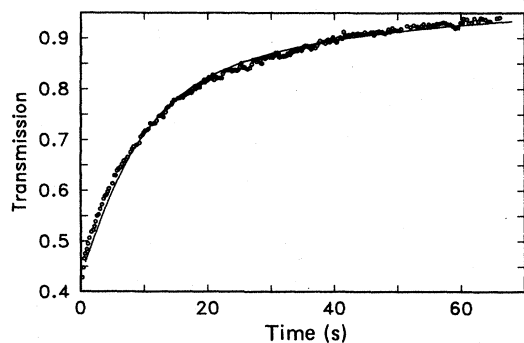
The values of these two parameters used for Fig. 6 were $\sigma=4.8\times10^{-13}$ cm^2 and $\eta_P=2.3\times10^{-2}$, and variations of these parameters over a 10% range produced clearly unacceptable fits. The agreement between this kinetic model and the experimental growth curve is striking. In addition, the values of the two adjustable parameters agree fairly well with the values of σ and η estimated by other methods presented earlier in this paper. We may conclude that our first-order photochemical model that assumes a constant quantum efficiency for all centers is quite appropriate for photochemical hole burning in the 8892-Å color center.

Further evidence for the applicability of our model results from a consideration of the hole line shape as a function of burning time. To compute the hole line shape, we leave the center of the hole at $\omega=0$ and assume that the sample is probed with a low-power tunable laser with frequency ω'. At any instant in time, the flux in the probing beam $F'(x,t,\omega')$ is governed by the following local propagation equation:

$$\frac{dF'(x,t,\omega')}{dx}$$

$$=-\sigma\left[\frac{\Gamma}{\pi}\int_{-\infty}^{\infty}\frac{d\omega}{\Gamma^2+(\omega-\omega')^2}N(x,t,\omega)\right]F'(x,t,\omega'),$$

(5)

where once again the inhomogeneous line has been assumed to be featureless for the range of ω values in which the integrand is appreciable. The solution to Eq. (5) was computed using Adams-Moulton predictor-corrector methods for several "time snapshots," in order to produce the hole line shapes presented in Fig. 7. The parameters used in this integration procedure were identical to those used to produce Fig. 6. The hole broadening that occurs with extended burning times is clearly evident in the figure. The measured hole widths stated in Fig. 5 agree within experimental uncertainty with the computed hole line shapes in Fig. 7, giving further evidence that a first-order, constant$_0$ quantum efficiency model is appropriate for the 8892-Å color center hole-burning mechanism. (The signal-to-noise ratio of the hole spectra did not per-

FIG. 6. Comparison of measured and computed values of the sample transmission as a function of burning time. The solid curve represents the prediction of the first-order kinetic model described in the text, and the circles represent a digitization of the sample transmission shown in Fig. 5.
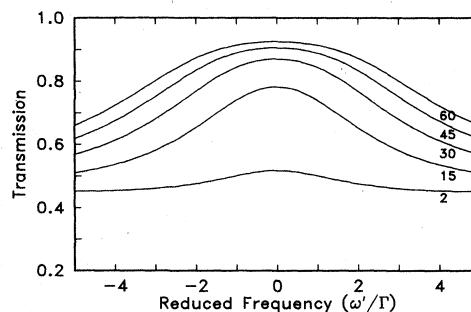
FIG. 7. Hole line shapes in transmission as a function of reduced probe laser frequency, ω'/Γ. The various curves correspond to "snapshots" at the time indicated in seconds from the start of burning.

mit further fitting of the observed line shapes; future measurements may address this problem in order to test the model more strongly.)

Supposing that the burning process is photoinduced electron tunneling, we may therefore expect that the barrier for electron release is depressed in a similar fashion for all centers due to the presence of nearby traps of unknown nature. The distribution of traps must yield a fairly narrow distribution of barrier heights in order for the data to fit a constant quantum efficiency model so well. It is hoped that future theoretical efforts will consider this problem, and that Stark and uniaxial stress experiments will be performed to establish the local symmetry of this center and investigate the trapping mechanism.

Hole burning in the NaF:OH$^-$ color center at 8892 Å has been shown to be efficient for burning at low powers with burning times on the order of seconds. The question remains, can holes be burned in very short times at high powers? To test this, a series of experiments were performed in which the hole depths were measured for constant energy exposures over a wide range of burning times. Experiments in the short time range can lead to the discovery of more details of the hole-burning mechanism, such as the presence of long-lived intermediate states, or bottlenecks.[23,24] We chose a burning energy of roughly 10 μJ, which produces a deep hole (nearly 100% deep) at long (i.e., seconds) burning time and low power. As the burning time was reduced below 100 ms, the hole depth was observed to decrease, until for times less than 1 ms, the holes were unobservable (i.e., less than 3—5 % deep). These results imply the presence of a bottleneck in the burning cycle in the 1-ms range. A similar phenomenon has been observed for the system composed of free-base phthalocyanine in polymer matrices.[23,24] The origin of the bottleneck in the 8892-Å color-center hole burning is unknown at present. It may be due to intersystem crossing into long-lived triplet states, for example. In such a situation, the vibrational energy released during relaxation after intersystem crossing provides the energy to overcome the barrier to electron tunneling. Since only holes of

relative depth equal to η can be burned in short times, the bottleneck for this material represents a limitation for frequency-domain optical storage applications, unless techniques can be found for the detection of very shallow holes at low probe beam intensity.[24]

In summary, we have described the properties of a new material for spectral hole burning, the 8892-Å color center in NaF:OH$^-$ and NaF:Mn^{2+}. No difference in the hole formation process was observed between the two dopant ions. The inhomogeneous linewidth increases with increasing OH$^-$ concentration, but the low-power hole linewidth remains at the value 1.65±0.15 GHz independent of the OH$^-$ concentration. The hole-growth dynamics including growth curves and linewidths can be well described by a first-order kinetic model with a constant quantum efficiency for all centers, if the influence of near-resonant centers and spatial variation of the intensity are taken into account. An approximate value of the quantum efficiency has been determined to be roughly 1.5×10^{-2}, which proves that low quantum efficiency hole burning is not a universal characteristic of color centers. For burning at low powers and long times, holes may be burned 100% deep, but for burning in the submillisecond time regime at high powers, a bottleneck in the burning cycle limits the attainable hole depth to values less than a few percent. The hole-burning mechanism is presumably the tunneling of an electron to a deep nearby trap, but further research on the dynamics of this new color center is necessary to identify the exact process.

ACKNOWLEDGMENTS

[1]G. Castro, D. Haarer, R. M. Macfarlane, and H. P. Trommsdorff, U.S. Patent No. 4 101 976, 1978 (unpublished); D. Haarer, Proc. Soc. Photo-Opt. Instrum. Eng. 177, 97 (1979); C. Ortiz, R. M. Macfarlane, R. M. Shelby, W. Lenth, and G. C. Bjorklund, Appl. Phys. 25, 87 (1981).

[2]L. A. Rebane, A. A. Gorokhovskii, and J. V. Kikas, Appl. Phys. B 29, 235 (1982).

[3]W. E. Moerner, A. J. Sievers, R. H. Silsbee, A. R. Chraplyvy, and D. K. Lambert, Phys. Rev. Lett. 49, 398 (1982); W. E. Moerner, A. R. Chraplyvy, A. J. Sievers, and R. H. Silsbee, Phys. Rev. B 28, 7244 (1983).

[4]S. Völker, R. M. Macfarlane, A. Z. Genack, H. P. Trommsdorf, and J. H. van der Waals, J. Chem. Phys. 67, 1759 (1977).

[5]For a review, see D. B. Fitchen, in Physics of Color Centers, edited by W. B. Fowler (Academic, New York, 1968), pp. 293—350.

[6]R. M. Macfarlane and R. M. Shelby, Phys. Rev. Lett. 42, 788 (1979).

[7]M. D. Levenson, R. M. Macfarlane, and R. M. Shelby, Phys. Rev. B 22, 4915 (1980).

[8]R. M. Macfarlane, R. T. Harley, and R. M. Shelby, Radiat. Effects 72, 1 (1983).

[9]W. E. Moerner, F. M. Schellenberg, and G. C. Bjorklund, Appl. Phys. B 28, 263 (1982); W. E. Moerner, P. Pokrowsky, F. M. Schellenberg, and G. C. Bjorklund (unpublished).

[10]P. Pokrowsky, W. E. Moerner, F. Chu, and G. C. Bjorklund, Opt. Lett. 8, 280 (1983).

[11]The system composed of nitrogen defects in diamond may have efficiencies in the range 10^{-2} to 10^{-4}. See R. T. Harley, M. J. Henderson, and R. M. Macfarlane, J. Phys. C 17, L233 (1984).

[12]For a description of the methods used here for the estimation of hole-burning quantum efficiencies, see W. E. Moerner, M.

Gehrtz, and A. L. Huston, J. Phys. Chem. **88**, 6459 (1984) and Ref. 3.

[13]A preliminary report of this work has already been presented; see P. Kaipa, F. Lüty, G. C. Bjorklund, and W. E. Moerner, Bull. Am. Phys. Soc. **28**, 451 (1983).

[14]P. Kaipa and F. Lüty, preceding paper, Phys. Rev. B **32**, 1264 (1985).

[15]The only other color center showing production of 100% deep holes is the 5770-Å color center in x-irradiated NaF. See R. T. Harley and R. M. Macfarlane, J. Phys. C **16**, L395 (1983).

[16]D. E. Horne and W. E. Moerner (unpublished).

[17]H. de Vries and D. A. Wiersma, J. Chem. Phys. **72**, 1851 (1980).

[18]W. Beall Fowler, in *Physics of Color Centers*, edited by W. B. Fowler (Academic, New York, 1968), pp. 627 and 628.

[19]E. L. Simmons, J. Phys. Chem. **75**, 588 (1971).

[20]We use η_P here rather than η because the two measures of quantum efficiency are not exactly equivalent. η is defined by basic physical arguments (see Ref. 12) and measures the effective quantum efficiency for all centers within a homogeneous linewidth of the laser wavelength. In the definition of η, the fact that excitation rate depends upon detuning has only been approximated. η_P is the peak quantum efficiency for those centers exactly in resonance, as defined by the frequency-dependent model of Eq. (3). It has been pointed out to us by K. Bløtekjaer (unpublished) that Eqs. (3) and (4) may be used to show that $\eta_P = 2\eta$. Since it is seldom possible to measure quantum efficiency to better than a factor of 2, these two definitions are essentially equivalent in practice.

[21]P. Kolodner, H. S. Kwok, J. G. Black, and E. Yablonovitch, Opt. Lett. **4**, 38 (1979).

[22]R. W. Olson, H. W. H. Lee, F. G. Patterson, and M. D. Fayer, J. Chem. Phys. **76**, 31 (1982).

[23]W. E. Moerner, in *Proceedings of the International Conference on Lasers '83*, edited by R. C. Powell (STS, McLean, Virginia, 1983), p. 489.

[24]M. Romagnoli, W. E. Moerner, F. M. Schellenberg, M. D. Levenson, and G. C. Bjorklund, J. Opt. Soc. Am. B: Opt. Phys. **1**, 341 (1984).